



US Army Corps  
of Engineers®

# Representation of Nonerodible (Hard) Bottom in Two-Dimensional Morphology Change Models

*by Hans Hanson and Adele Militello*

**PURPOSE:** This Coastal and Hydraulics Engineering Technical Note (CHETN) describes a methodology for representing nonerodible substrates in a two-dimensional (2-D) coastal morphology change models, with emphasis on coastal inlets. The calculation procedure is described, followed by examples showing the functioning of the method.

**BACKGROUND:** Morphology change models apply sediment transport formulas to calculate transport rates from which depth change is computed. Predictive sediment transport formulas are based on the presumption that there is sediment available corresponding to the transport capacity of the hydrodynamic forcing. At many coastal inlets, however, the sea bottom may be covered by hard or nonerodible material, which may or may not be covered by a layer of sediment. Hard-bottom location and composition are determined by geotechnical surveys such as coring, beach profiling and hydrographic surveying, diver inspection, and aerial photographs. Various forms of hard bottom are commonly encountered, imposing challenges for morphological modeling. Hard bottom may consist of material such as limestone, coral reef, sedimentary rock, submerged coastal structures such as jetty weirs, or even artificial material such as concrete. Figure 1 shows an example of a beach with rock outcrops extending from the shore into the inner surf zone. Sebastian Inlet, FL, shown in Figure 2, was blasted out of limestone, yielding an inlet that passes through an almost completely hard substrate. Exposed hard bottom is observed as darker bands under the water.

If hard bottom is exposed, the actual transport rate will be less than the potential (predicted by a transport relationship). With less mobile sediment leaving the exposed area, transport rates in surrounding regions will be influenced by the presence of neighboring hard bottom even though these areas may have sediment available for transport. In this way, hard-bottom areas will promote erosion or reduced accumulation in surrounding areas with erodible bottom because the availability of sand is reduced. Exposed hard bottom, thus, constitutes a constraint on the sediment transport and associated bottom change to be calculated.

A methodology was developed for representing hard bottom in 2-D morphology change models. The method applies a recalculation technique for transport rates at locations that are nonerodible and nearby areas, subject to certain principles discussed in this CHETN.

**BASIC PRINCIPLES:** The hard-bottom routine is a 2-D extension of the one-dimensional (1-D) methodology applied in the shoreline change model GENESIS (Hanson 1989) to represent the control of seawalls on longshore sediment transport and shoreline evolution (Hanson and Kraus 1985, 1986). The methodology was also applied by Kraus and Larson (1998) and Larson and Kraus (2000) to simulate cross-shore sediment transport and beach profile evolution in the presence of hard bottom in the SBEACH model (Larson and Kraus 1998).



Figure 1. Beach with outcrops of hard material in inner surf zone



Figure 2. Sebastian Inlet, FL

A hard bottom is a nonerodible surface that imposes a constraint on the sediment transport rate and water depth because the bottom cannot erode below the level of the existing surface. The procedure that has been developed is based on the following four principles (Hanson and Kraus 1985, 1986):

- a.* The sea bottom in areas with hard bottom cannot erode below the level of the hard bottom.
- b.* Sediment volume is conserved.
- c.* The direction of sediment transport at a location with hard bottom is the same as that of the potential local transport.
- d.* Correction to transport rates is done in the direction of potential sediment transport.

**SCHEMATIC PROCEDURE:** In any calculation cell where the potential transport rates (rates are calculated in two horizontal directions in a 2-D model) would cause the hard bottom to be exposed, the rates need to be reduced because of limited available quantity of sediment. In the methodology, this reduction is accomplished through a correction procedure. The following section explains how this correction is performed through successive loops in a hierarchic and systematic order. Although the basic principles are straight-forward, the calculation procedure is complex. For a detailed description of the associated 1-D analogy with the impact of a seawall on shoreline evolution, the reader is referred to Hanson and Kraus (1986).

First, sediment transport rates are calculated along the sea bottom based on the assumption that the calculated amount of sand is available for transport (the potential transport rate). These rates are then passed to the hard-bottom routine. At grid cells where the hard-bottom constraint is violated (i.e., the bottom is calculated to erode below the allowable hard-bottom level), the bottom level and all affected transport rates are adjusted. The presence of a hard bottom in a particular cell does not impose any restriction on transport into the cell. As the hard bottom becomes exposed, however, the transport out of the cell may need to be reduced. Neighboring cells receiving these reduced transport rates will then also be affected. As a consequence, transport rates and volume change in all neighboring downdrift cells are also adjusted, as necessary, to preserve sediment volume and the direction of transport.

Thus, the algorithm searches for cells from where the hard-bottom exposure originates. Then, the corrections are carried in the direction of transport. The basic procedure of the hard-bottom correction methodology is as follows:

- a.* Identify all cells with the transport across all four boundaries directed out of the cell. These cells are called “Minus4” cells because transport is outward on all four sides. These types of cells, if they are present, constitute the first (highest) level in the correction hierarchic procedure as they only provide sediment to adjacent cells and are not recipients of sediment.
- b.* If hard bottom is exposed, all transport rates out of the Minus4 cells are reduced. Thus, the hard-bottom calculation routine stores the locations of all adjacent, downdrift cells with or without hard bottom for later recalculation. These cells then constitute the second level in the correction procedure.

- c. Next, all downdrift adjacent cells are recalculated as a result of the reduced influx of sediment. Cells with hard bottom must then be checked for a possible violation of the hard-bottom constraint and corrected as necessary. For each corrected cell, all transport rates out of the cell are in turn corrected, and each of the next generation of affected cells adjacent to the corrected cell is added to the list of cells to be corrected. Transport rates are always changed in a cell where they constitute an outgoing transport rate.
- d. Once all Minus4 hierarchies have been investigated and corrected (or if there are no Minus4 cells), all remaining cells are checked to find “Start” cells of additional correction hierarchies. A Start cell is located on a hard bottom but not receiving sediment from any other hard-bottom cells. From these Start cells, correction is made in the same manner outlined for Minus4 cells.
- e. After the transport rates and bottom change at all cells have been adjusted, the process is reiterated to make sure that the hard-bottom constraint is not violated in any cell.

Through this method, cells will always be corrected in a hierarchic order where all cells at a higher level are corrected before proceeding to the lower level. The procedure ensures that corrections are performed in the direction of transport without ambiguity regarding which cell affects others.

**GOVERNING RELATIONSHIPS:** The change of elevation in a cell (Figure 3) follows the rule of continuity as:

$$D_{i,j}'' = D_{i,j}' + (qx_{i+1,j} - qx_{i,j}) \frac{dt}{dx} + (qy_{i,j+1} - qy_{i,j}) \frac{dt}{dy} \quad (1)$$

where  $D_{i,j}'$  (m) is the (positive) water depth at the old time-step at grid coordinates  $i$  and  $j$ ,  $D_{i,j}''$  (m) is the water depth at the new time-step,  $dt$  (s) is the calculation time-step,  $dx$  (m) is the cell length in the x-direction,  $dy$  (m) is the cell length in the y-direction,  $qx$  ( $m^3/m/sec$ ) is the transport rate in the x-direction, and  $qy$  ( $m^3/m/sec$ ) is the transport rate in the y-direction.

If  $D_{i,j}''$  becomes greater than (below) the hard-bottom level  $D_{hb,i,j}$ , the outgoing transport rates have to be corrected to match the criterion  $D_{i,j}'' = D_{hb,i,j}$ . Over one time-step, the total amount  $Vol_{out}$  ( $m^3$ ) that may leave the cell without violating the hard-bottom constraint is

$$Vol_{out} = (D_{hb,i,j} - D_{i,j}') dx dy + Q_{in} dt \quad (2)$$

where  $Q_{in}$  is the total influx ( $m^3/sec$ ) of sediment (inflowing  $qx$  and  $qy$  values) from the cell during the time-step. The correction factor  $K$  is given as

$$K = \frac{Vol_{out}}{Q_{out} dt} \quad (3)$$

where  $Q_{out}$  is the total outflux ( $m^3/sec$ ) of sediment (outflowing  $qx$  and  $qy$  values) from the cell during the time-step. To ensure that  $D_{i,j}'' = D_{hb,i,j}$ , all ingoing transport rates are left unchanged while

all outgoing transport rates are multiplied by the correction factor  $K$ . Thus, in Figure 3, outgoing transport rates  $qx_{i+1,j}$  and  $qy_{i,j+1}$  are replaced by  $K qx_{i+1,j}$  and  $K qy_{i,j+1}$ , respectively, if the hard bottom is exposed during the time-step.

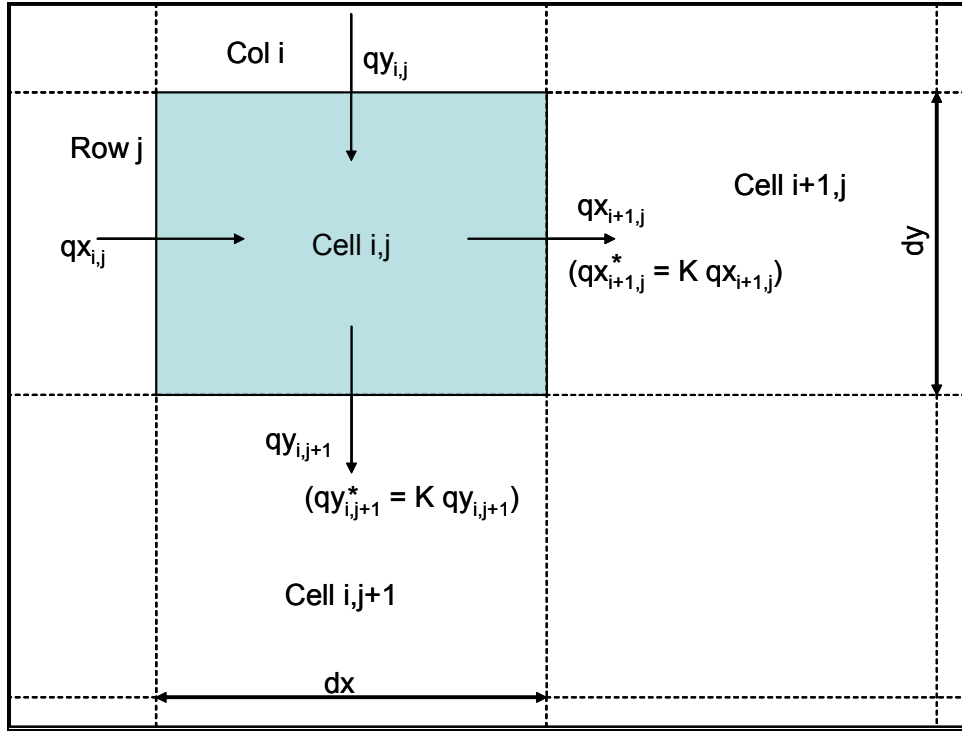


Figure 3. Schematic layout of cells, rows, columns, and transport rate sign convention

**APPLICATION EXAMPLES:** Examples of the functioning of the hard-bottom method are presented here. For each example, the modeling package applied to conduct the simulation is the Coastal Inlet Research Program’s (CIRP’s) Inlet Modeling System (IMS). This system comprises a modularized set of circulation and wave models that can be set up and run within the Surface-Water Modeling System (SMS). Two circulation models are available: IMS-M2D (Militello et al. 2004) is a 2-D finite-difference circulation and morphology change model that is designed for project-scale applications; IMS-ADCIRC (Luettich et al. 1992) is a 2-D finite-element circulation model that is primarily applied to regional-scale applications. Wave modeling in the IMS is conducted with the steady spectral wave model STWAVE (Smith et al. 2001). Coupling between circulation and wave models is conducted through the Steering Module of the SMS, which allows the user to control how and when the models are linked.

The hard-bottom algorithm was implemented into IMS-M2D. All application examples provided herein were conducted with IMS-M2D, in which the predictive formula of Watanabe (1987) was applied to compute sediment transport rates. (Additional sediment transport formulae are represented in IMS-M2D, but were not applied in these examples.) The IMS-M2D interface within the SMS allows the user to specify cells as hard bottom, as well as the depth of the hard substrate, which provides for hard-bottom areas to be initially covered with sand. The roughness of hard substrate can

differ from that of sand. Variable Manning's coefficients for M2D can be specified within the IMS-M2D interface.

**APPLICATION EXAMPLE 1 – COMPARISON OF SOLUTIONS WITH AND WITHOUT HARD-BOTTOM REPRESENTATION:** Example 1 was designed to demonstrate that the hard-bottom algorithm does not allow erosion of hard substrate, but does allow accumulation of sand over the nonerrodible surface. This example also demonstrates symmetry of the methodology and represents complex configurations of nonerrodible cells. The bathymetric configuration (Figure 4) was specified to be a plane horizontal bottom with a pyramid-shaped shoal in the center. The configuration was subject to sediment transport generated by a constant and uniform current in four different simulations where the current originated from each of the four sides of the square. If the hard-bottom routine is working properly, all simulations should give the same symmetrical result relative to the main current direction.

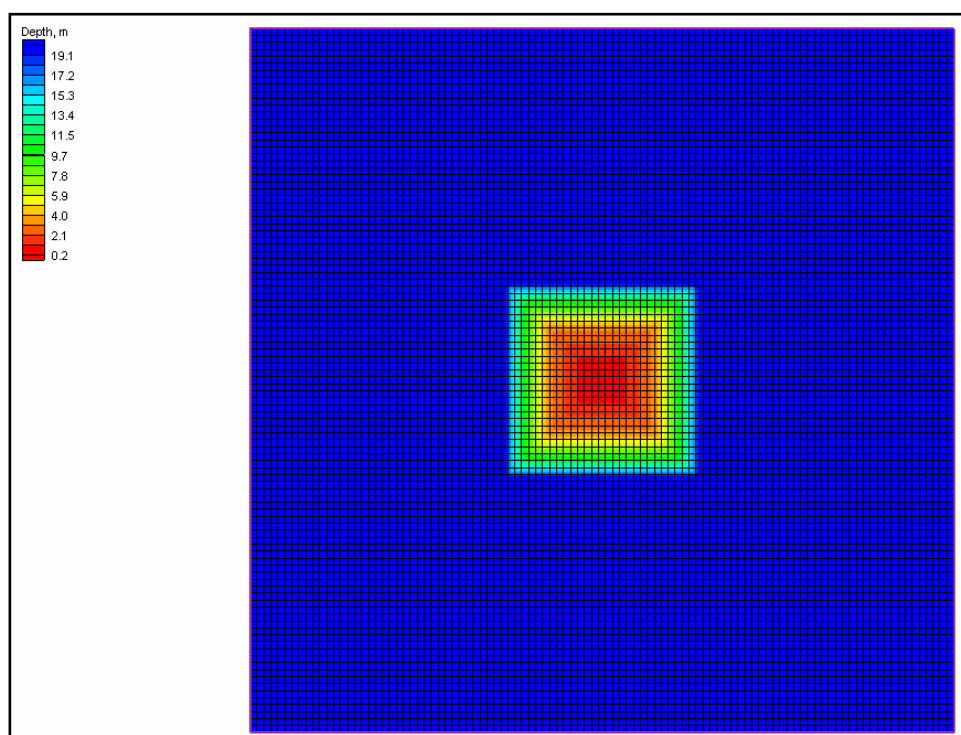


Figure 4. Model bathymetry with cells shown

Figure 5 shows the simulation where the current is coming from the left side. Because of the presence of the pyramidal sediment mound, the current bends around the structure as indicated in the figure. Under the influence of the current, the pyramid erodes.

Figure 6 shows a magnification of the center of the grid. Cells with triangles are specified as having a nonerrodible bottom at the initial cell depth (no sediment cover on the hard-bottom layer). Two sets of runs are compared. In the first set, the hard bottom is not in place, i.e., allowing the cells to erode. In the second set, the hard-bottom cells are in place, limiting erosion to a specified hard-bottom depth. Erosion below the hard-bottom level is allowed in these cells during the first set of runs, but not during the second set.

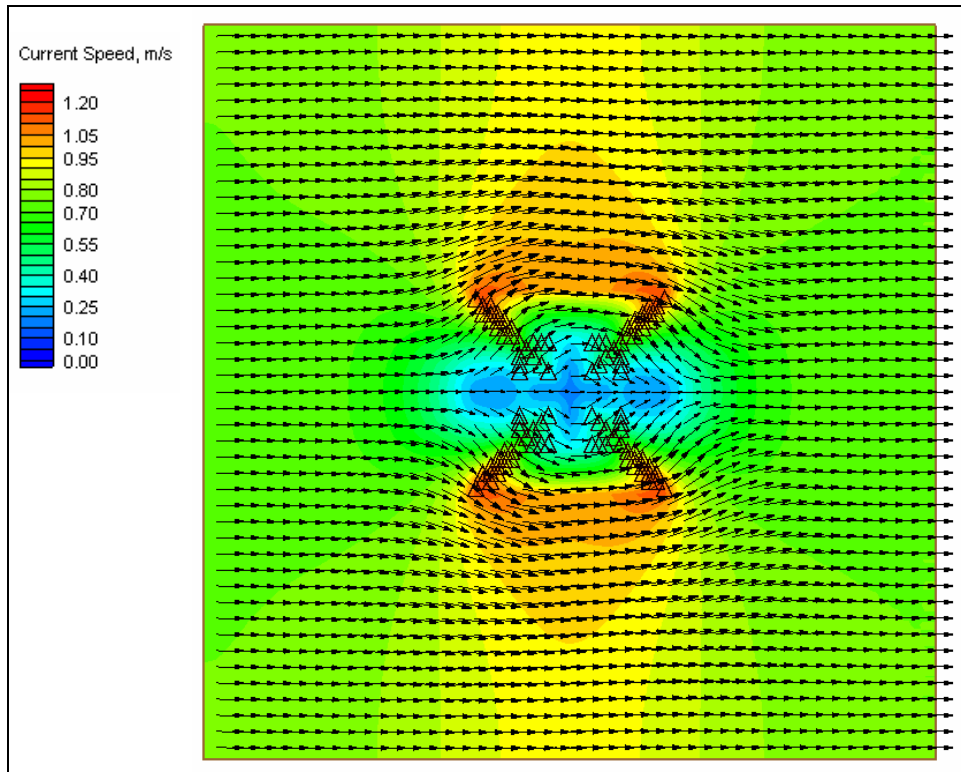


Figure 5. Velocity field over schematized bottom

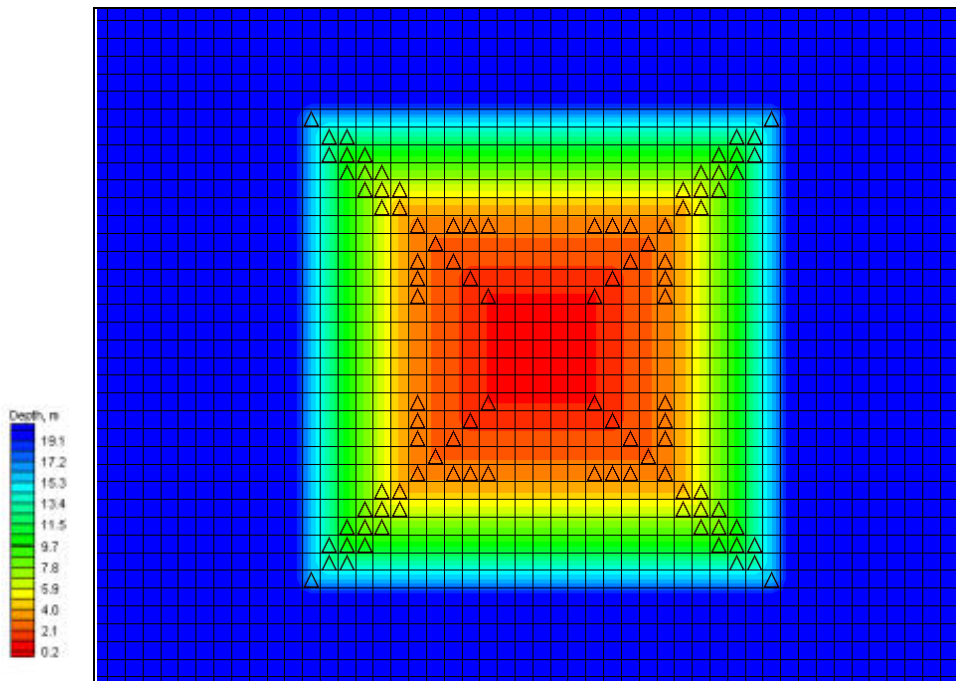


Figure 6. Magnification of bathymetry at center of grid. Cells with triangles are specified as having hard nonerodible bottom (Color code same as for Figure 2)

The result of this comparison is shown in Figure 7 displaying the change in depth (blue denotes erosion, and yellow/red denote accretion) after 7 hr of simulation with no hard-bottom cells present (triangles are retained in the image for reference to previous figure). Cells that have hard bottom in the next set of simulation are now eroding, indicating that the hydrodynamic conditions cause the bottom to erode below the level of the hard bottom to be used in the next set. The depth change pattern is symmetric. Figure 8 shows the same situation, but now with the hard bottom in place. The calculations show that there is no erosion below the hard-bottom cells. Also, symmetry is preserved.

Although not shown here, other simulations with the current originating from the other three sides of the square gave the same symmetrical results relative to the main current direction. In all simulations, sand volume was conserved.

### APPLICATION EXAMPLE 2 – EROSION AND ACCRETION OF SAND OVER HARD

**BOTTOM:** A computational grid was developed representing a canal with a shallow region located in its center (Figure 9). Grid depths vary along the x-axis and are uniform along the y-axis. In Figure 9, cells having hard substrates are denoted with triangles. During the simulation, these cells will erode to the hard bottom surface, then undergo deposition and erosion. The hard-bottom depth was specified to be 0.7 m and initial grid depths at these cells were 0.5 m, meaning that 0.2 m of sand covered the hard substrate at the beginning of the simulation. The sand size was specified to be 0.2 mm.

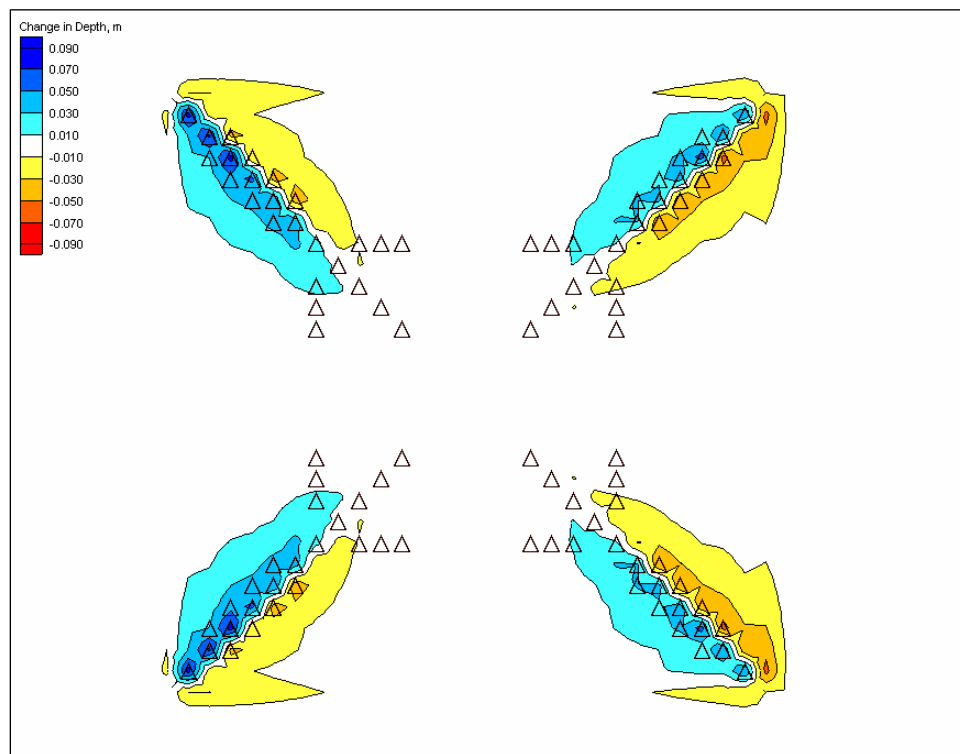


Figure 7. Change in depth after 7 hr of simulation *without* hard-bottom cells (triangles are left in image for reference to previous figure). Blue denotes erosion; yellow/red denote accretion

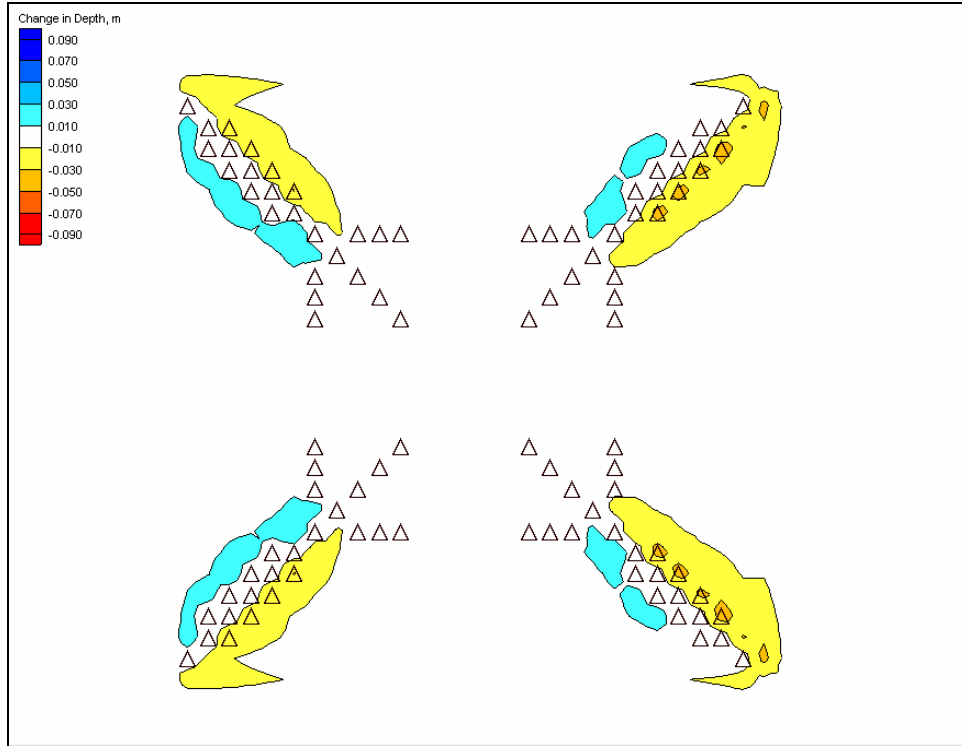


Figure 8. Change in depth after 7 hr of simulation *with* hard bottom cells. Blue denotes erosion and yellow/red denote accretion

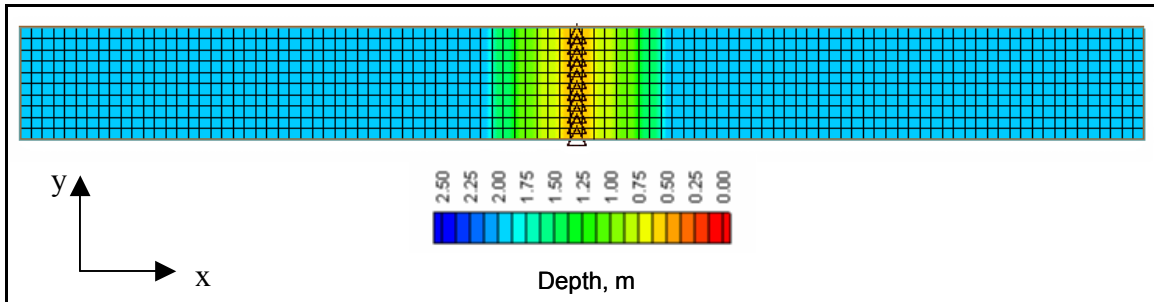


Figure 9. Computational grid and bathymetry for demonstration of erosion and deposition of sand over hard substrate. Triangles denote hard-bottom cells

A 400-hr simulation was conducted in which the current flowed to the right (positive) for 200 hr and then to the left (negative) for 200 hr, providing conditions for both erosion and deposition at the hard-bottom cells. Time series of current velocity and depth at one hard-bottom cell are shown in Figure 10. During the first 90 hr of the simulation, scour of the sand layer takes place. Once the hard-bottom substrate is reached, scour ceases and the depth remains constant at 0.7 m until current velocities are weak enough for shoaling to start (approximately hour 210). Sand accumulates until the current is strong enough to begin erosion (approximately hour 280), and the erosion continues until the hard substrate is reached again. Thus, the hard-bottom algorithm functions correctly for situations in which sand overlays the hard substrate and erosion takes place to the level of the hard bottom, and for situations in which conditions become depositional at hard-bottom cells.

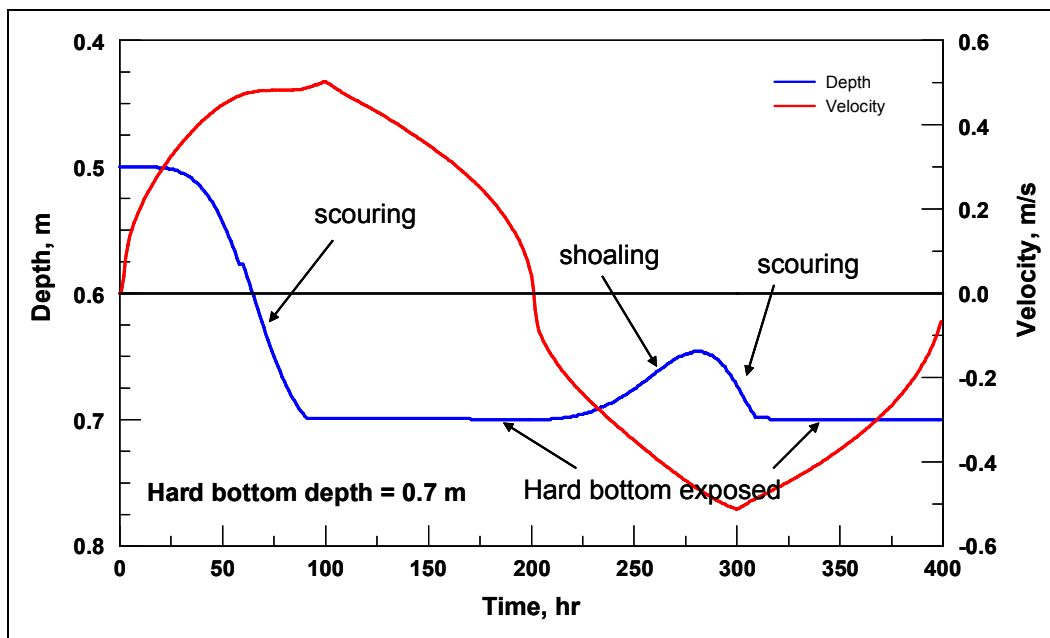


Figure 10. Time series of depth of bottom and velocity for demonstration of scour and accumulation of sand over hard substrate

**APPLICATION EXAMPLE 3 - SEBASTIAN INLET, FL:** The east coast of Florida has several regions where a nonerrodible substrate is present. These regions typically consist of linear rock reef features and exposed limestone outcrops. Sebastian Inlet, located on Florida's central east coast, was cut through limestone, and much of the inlet bottom is nonerrodible. Figure 11 is an aerial photograph of the inlet with exposed hard-bottom shown in pink. The area of hard bottom at Sebastian Inlet is located not only within the inlet, but also in the nearshore south of the inlet. Demonstration of the hard-bottom representation is presented here for Sebastian Inlet to provide a realistic application. Simulations are conducted with and without hard-bottom cells specified in the model, and comparisons of resulting bottom change calculations are made.

A computational grid for IMS-M2D was developed that included Sebastian Inlet, the Atlantic Ocean in the vicinity of the inlet, and a portion of the Indian River Lagoon. The grid was composed of 8,575 computational cells having maximum cell dimension of 100 m and minimum cell dimension of 10 m. Figure 12 shows the IMS-M2D bathymetry and computational grid. An STWAVE grid was developed from the same bathymetry to calculate waves in the ocean and through the inlet. The STWAVE grid had a cell spacing of 20 m.

STWAVE was forced with a time series of wave height, period, and direction, with heights ranging from 0.4 to 1.5 m and directions ranging from -20 to 20 deg relative to shore normal. IMS-M2D boundaries at the ocean and north and south ends of the lagoon were forced with time series of measured water levels. Simulations were conducted with the SMS Steering Module, which allows coupling of IMS-M2D and STWAVE, and calculation of wave-driven currents. The models were coupled every 3 hr, and the total simulation time was 81 hr.



Figure 11. Hard-bottom regions (pink) of Sebastian Inlet and adjacent nearshore area (Image courtesy of Dr. Gary A. Zarillo, Florida Institute of Technology)

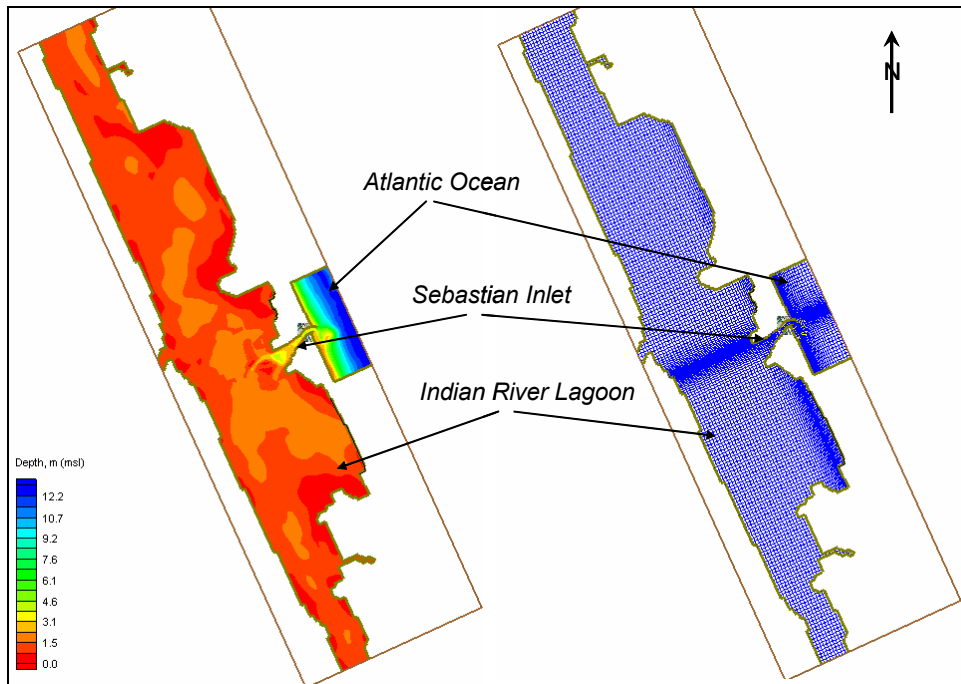


Figure 12. Sebastian Inlet model bathymetry (left) and grid (right)

Two simulations were conducted. The first simulation did not specify hard-bottom cells. In the second simulation, hard-bottom cells were specified according to the coverage shown in Figure 11.

Examples of peak flood and ebb currents through Sebastian Inlet are shown in Figures 13 and 14, respectively. During flood tide, currents exceeding 1 m/sec are present over a large portion of the inlet. During ebb tide, currents exceeding 1 m/sec are present over a smaller portion of the inlet, and a well-formed jet extends seaward of the jetties. Wave-induced currents form from wave breaking on the ebb shoal during both flood and ebb tide.

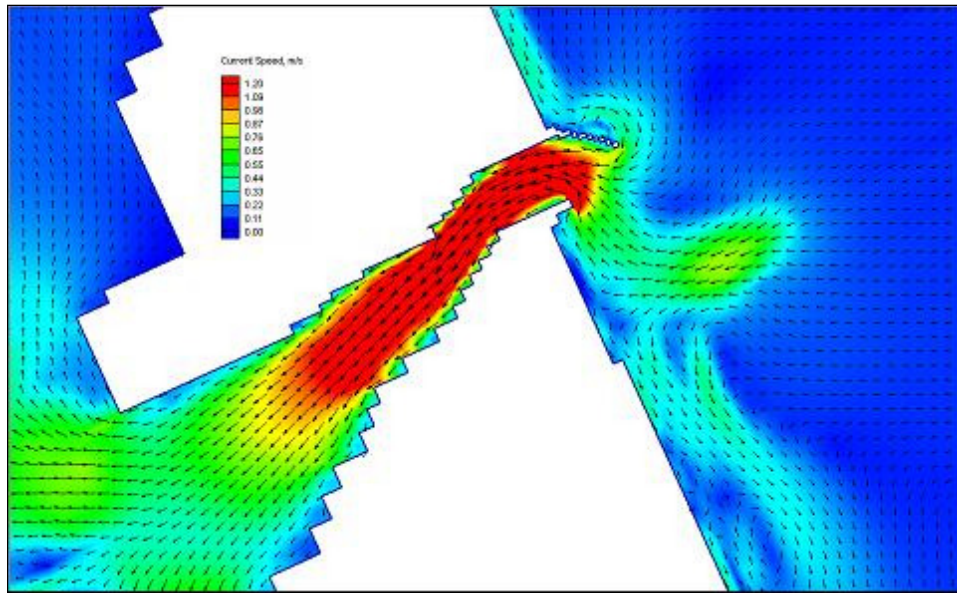


Figure 13. Peak flood current through Sebastian Inlet

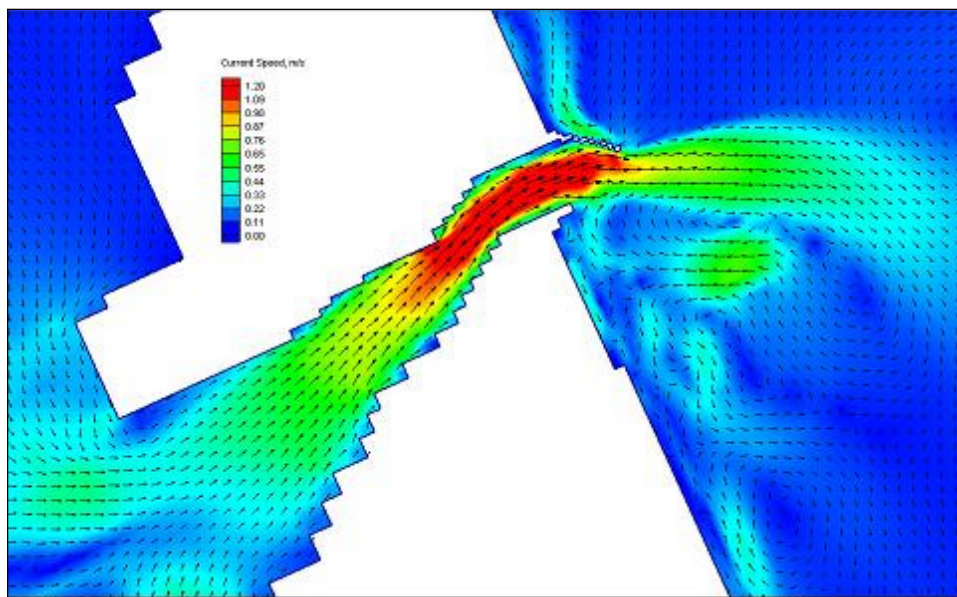


Figure 14. Peak ebb current through Sebastian Inlet

Computed depth change after 81 hr of simulation is shown for the calculation without representation of hard bottom (Figure 15). Positive depth change, shown in blue, denotes erosion, and negative depth change shown in yellow and red, denotes deposition. Without representation of the non-erodable substrate, greatest erosion takes place at the south jetty tip and along the flanks of the inlet in its middle section. Deposition takes place directly adjacent to the south jetty tip, and along the central inlet thalweg. On the northern portion of the inlet, between the entrance and narrowest portion, regions of both erosion and accretion are present.

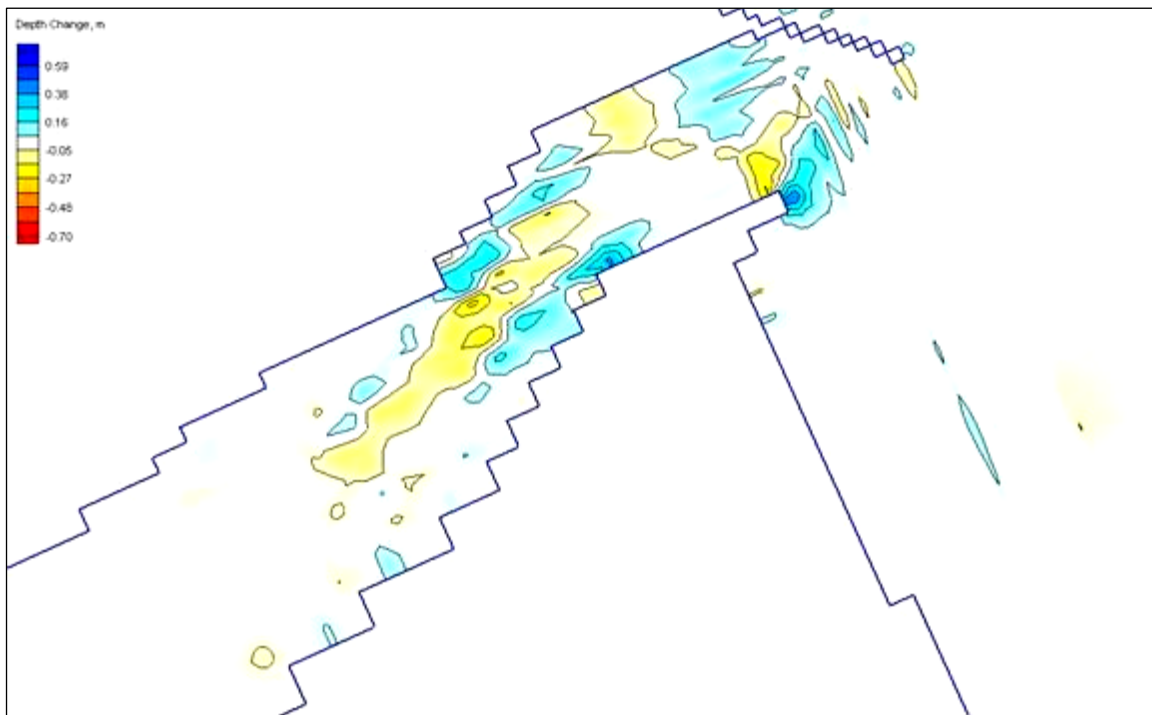


Figure 15. Depth change after 81 hr without hard bottom represented

Computed depth change after 81 hr of simulation is shown in Figure 16 for the calculation with representation of hard bottom (hard-bottom cells are denoted by triangles). With hard bottom represented, the erosion and accretion patterns are significantly different from the simulation without such representation. At the tip of the south jetty, deposition takes place rather than erosion. Hard-bottom cells are seen to be accretionary in several locations, and no hard-bottom cells erode (Note that some hard-bottom cells are shown in light blue, but actually have depth change values of zero. The blue in these areas is an artifact of the contouring algorithm.). Areas of greatest erosion are located in the interior flanks of the inlet, but the accretionary area in the thalweg that was computed without representation of hard bottom is now absent. The differences in the two simulations demonstrate that cells represented as hard bottom do not erode, but can accrete. Also, with hard substrate represented, material that would have been transported owing to allowed erosion without this representation, is no longer available. Thus, in the simulation with hard-bottom representation, sediment available for deposition in the channel thalweg was greatly reduced, as compared to the simulation that did not account for the hard bottom. This difference in sediment availability, together with preservation of the depth of the hard substrate, results in depth change patterns that vary substantially from simulations in which hard substrate is not taken into account.

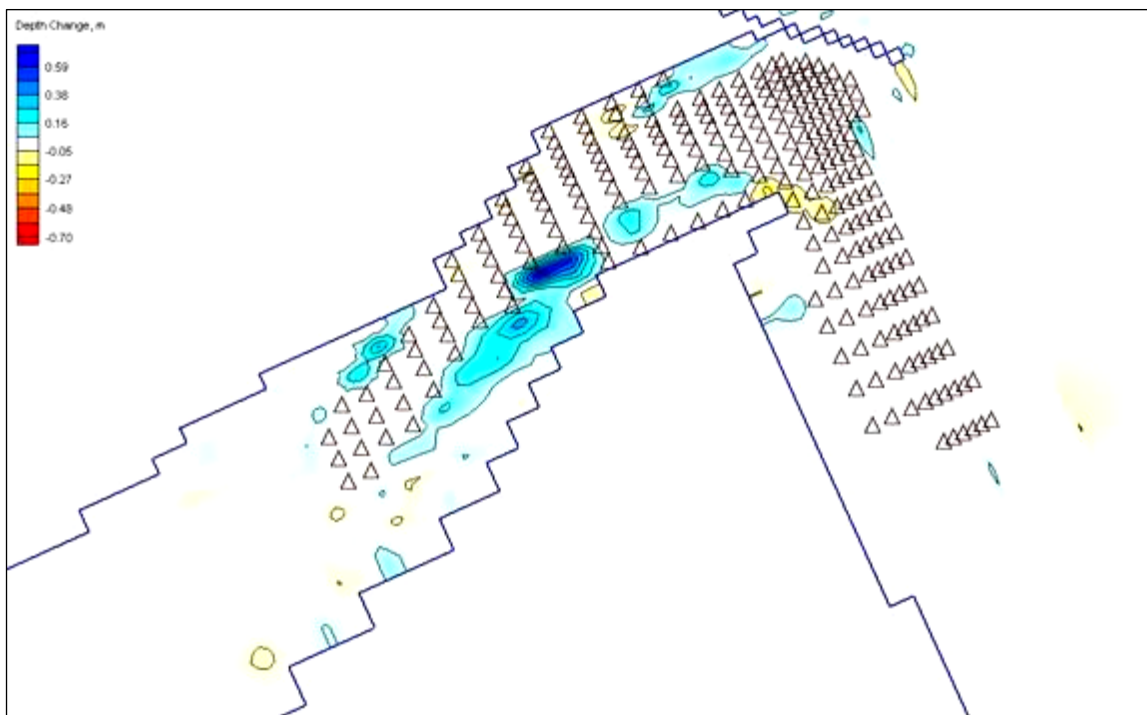


Figure 16. Depth change after 81 hr with hard bottom represented (triangles denote hard-bottom cells)

**ACKNOWLEDGEMENTS:** All bathymetric data, wave input, water-level data, and hard-bottom coverage (overlaid on aerial photograph) for the Sebastian Inlet example were provided by Dr. Gary A. Zarillo, Florida Institute of Technology. The photograph of beach rock outcrops and oblique photograph of Sebastian Inlet were taken by Dr. Nicholas Kraus, U.S. Army Engineer Research and Development Center. Dr. Kraus suggested this research project and provided encouragement through the course of the study.

**POINTS OF CONTACT:** Questions about this CHETN can be addressed to Dr. Hans Hanson at +46 46 222 8987 or [Hans.Hanson@tvrl.lth.se](mailto:Hans.Hanson@tvrl.lth.se), to Dr. Adele Militello at (707) 444-2173 or [CoastalAnalysis@cox.net](mailto:CoastalAnalysis@cox.net), or to Ms. Mary A. Cialone at (601) 634-2139 or [Mary.A.Cialone@erdc.usace.army.mil](mailto:Mary.A.Cialone@erdc.usace.army.mil). This CHETN was produced under the Inlet Modeling System work unit of the Coastal Inlets Research Program. For information about the Coastal Inlets Research Program, please contact the Program Manager, Dr. Nicholas C. Kraus, at (601) 634-2016 or [Nicholas.C.Kraus@erdc.usace.army.mil](mailto:Nicholas.C.Kraus@erdc.usace.army.mil).

## REFERENCES

- Hanson, H., and Kraus, N. C. (1985). "Seawall constraint in the shoreline numerical model," *Journal of Waterway, Port, Coastal and Ocean Engineering* 111(6), 1,079-1,083.
- Hanson, H., and Kraus, N. C. (1986). "Seawall boundary condition in numerical models of shoreline change," Technical Report CERC 86-3, Coastal Engineering Research Center, U.S. Army Engineer Waterways Experiment Station, Vicksburg, MS, 59 pp.
- Hanson, H. (1989). "GENESIS - A generalized shoreline change numerical model," *Journal of Coastal Research* 5(1), 1-27.

- Kraus, N. C., and Larson, M. (1998). "Numerical simulation of beach-profile change accounting for hard-bottom features," *Proceedings 11th National Conference on Beach Preservation Technology*, Florida Shore & Beach Preservation Association, Tallahassee, FL, 123-138.
- Larson, M., and Kraus, N. C. (1998). "SBEACH: Numerical model for simulating storm-induced beach change, Report 5: Representation of nonerodible (hard) bottoms," Technical Report CERC-89-9, Coastal Engineering Research Center, U.S. Army Engineer Waterways Experiment Station, Vicksburg, MS.
- Larson, M., and Kraus, N. C. (2000). "Representation of non-erodible (hard) bottoms in beach profile change modeling," *Journal of Coastal Research* 16(1), 1-14.
- Luetlich, R. A., Westerink, J. J., and Scheffner, N. W. (1992). "ADCIRC: An advanced three-dimensional circulation model for shelves, coasts, and estuaries; Report 1: Theory and methodology of ADCIRC-2DDI and ADCIRC-3DL," Dredging Research Program Technical Report DRP-92-6, U.S. Army Engineer Waterways Experiment Station, Vicksburg, MS.
- Militello, A., Reed, C. W., Zundel, A. K., and Kraus, N. C. (2004). "Two-dimensional circulation model M2D: Version 2.0, Report 1, technical documentation and user's guide," Coastal Inlets Research Program Technical Report ERDC-CHL-TR-04-02, U.S. Army Engineer Research and Development Center, Vicksburg, MS.
- Smith, J. M., Sherlock, A. R., and Resio, D. T. (2001). "STWAVE: STEady-state spectral WAVE model: User's manual for STWAVE Version 3.0," Supplemental Report ERDC/CHL SR-01-1, U.S. Army Engineer Research and Development Center, Vicksburg, MS.
- Watanabe, A. (1987). "3-dimensional numerical model of beach evolution," *Proceedings Coastal Sediments '87*, 802-817.

**NOTE:** *The contents of this technical note are not to be used for advertising, publication, or promotional purposes. Citation of trade names does not constitute an official endorsement or approval of the use of such products.*